Supporting Information

Rylene Annulated Subphthalocyanine: A Promising Cone-Shaped Non-Fullerene Acceptor for Organic Solar Cells

Tengda Huang,[†,#] Hui Chen,[§] Jiajing Feng,[‡] Andong Zhang,[‡] Wei Jiang,[*,†] Feng He,[*,§] and Zhaohui Wang[*,‡]

[†] CAS Research/Education Center for Excellence in Molecular Sciences, Institute of Chemistry, Chinese Academy of Sciences, Beijing 100190, People's Republic of China. Email: jiangwei@iccas.ac.cn
[‡] Key Laboratory of Organic Optoelectronics and Molecular Engineering, Department of Chemistry, Tsinghua University, Beijing 100084, China. Email: wangzhaohui@mail.tsinghua.edu.cn
[§] Department of Chemistry, Southern University of Science and Technology, Shenzhen 518055, People's Republic of China. Email: hef@sustc.edu.cn
[#] University of Chinese Academy of Sciences, Beijing 100049, People's Republic of China.

Table of Contents

1. Materials and Methods

All chemicals and solvents were purchased from commercial suppliers and used without further purification unless otherwise specified.

^{1}H NMR and ^{13}C NMR spectra were obtained in deuterated solvents on a Bruker ADVANCE 500 NMR Spectrometer. Chemical shifts are expressed in ppm using the residual protonated solvent as an internal standard. The signals have been named as follows: s (singlet), d (doublet), t (triplet), q (quartet), dd (doublet doublet) and m (multiplets). High resolution mass spectra (HRMS) were determined on IonSpec 4.7 Tesla Fourier Transform Mass Spectrometer. UV-vis-NIR absorption spectra were measured with Hitachi (Model U-3010) UV-vis spectrophotometer in a 1 cm quartz cell unless otherwise specified. Cyclic voltammograms (CVs) were recorded on a Zahner IM6e electrochemical workstation, with glassy carbon discs as the working electrode, Pt wire as the counter electrode, Ag/AgCl electrode as the reference electrode at a scanning rate of 100 mV/s. 0.1 M tetrabutylammoniumhexafluorophosphate (Bu_4NPF_6) dissolved in CH_2Cl_2 was used as the supporting electrolyte, which was calibrated by the redox couple of ferrocene/ferrocenium (Fc/Fc^+). Thermogravimetric analysis (TGA) measurements were performed on a TGA 8000 instrument under a dry nitrogen flow, heating from room temperature to 550 ºC, at a heating rate of 10 ºC/min. The room temperature optical absorption of the thin films was measured by using a UV-vis spectrophotometer (UV3600, SHIMADZU).

2. Synthesis and Characterization

SubPcPDI3-Cl:

A Schlenk flash charged with compound **1** (100 mg, 0.122 mmol), added 0.8 mL of *p*-xylene and 0.8 mL of BCl_3 (1 M solution in *p*-xylene) in drop-wise under an argon atmosphere. After stirring at room temperature for a few minutes, the mixture then reacted at 140 ºC for 2 h. After cooling to room temperature, the mixture was flushed with argon until the solvent was evaporated. The residue was purified by fast column chromatography with DCM/hexane = 2/1 as the eluent. The pure compound was further purified by using HPLC with DCM/hexane = 2.5/1 as eluent and 490 nm as detected wavelength to obtained dark-green solid (18 mg, 18%).

^{1}H NMR (500 MHz, $CD_2Cl_2CD_2Cl_2$, 373 K): δ = 11.20 (s, 6H), 10.75 (s, 6H), 9.26 (s, 6H), 9.17 (s, 6H), 5.53 (s, 6H); ^{13}C NMR (125 MHz, $CD_2Cl_2CD_2Cl_2$, 373 K): δ = 164.3, 149.3, 133.8, 131.0, 130.3, 129.3, 128.3, 127.8, 125.7, 124.7, 124.0, 123.4, 123.1, 119.2, 55.8, 32.8, 31.9, 29.6, 22.6, 22.5, 13.8. HRMS (MALDI, 100%): calcd (%) for $C_{162}H_{162}BClN_{12}O_{12}$: 2513.2244; found, 2513.2222.

SubPcPDI3-$OC_6H_4{}^tBu$:

A Schlenk flash was charged with **SubPcPDI3-Cl** (100 mg, 0.04 mmol), 4-*t*-butylphenol (35.8 mg, 0.24 mmol) under argon. Then 6 μL of DBU and 5 mL of toluene was added by injection, and the mixture reflexed for 8 h. After cooling to room temperature, the mixture was purified by silica gel column chromatography with DCM/hexane = 2/1 as the eluent to afford dark-green solid (52 mg, 50%).

^{1}H NMR (500 MHz, $CD_2Cl_2CD_2Cl_2$, 373 K): δ = 11.16 (s, 6H), 10.85 (s, 6H), 9.35 (s, 6H), 9.19-9.17 (d, *J*=8.0Hz, 6H), 6.94 (s, 2H), 5.71 (s, 2H), 5.53 (s, 6H); ^{13}C NMR (125 MHz, $CD_2Cl_2CD_2Cl_2$, 373 K): δ = 164.4, 150.9, 144.7, 134.2 130.7, 130.4, 130.3, 129.7, 128.9, 128.0, 126.1, 125.9, 125.1, 124.1, 123.5, 119.0, 118.4, 55.6, 32.8, 32.7, 31.9, 31.8, 31.4, 26.9, 22.6, 22.5, 13.9. HRMS (MALDI, 100%): calcd (%) for $C_{172}H_{175}BN_{12}O_{13}$: 2627.3522; found, 2627.3538.

3. Computational Details

The density functional theory (DFT) calculations[1] were performed with the Gaussian 09 Rev. E.01 quantum chemistry package at the B3LYP level employing the 6-31G (d, p) basis set.

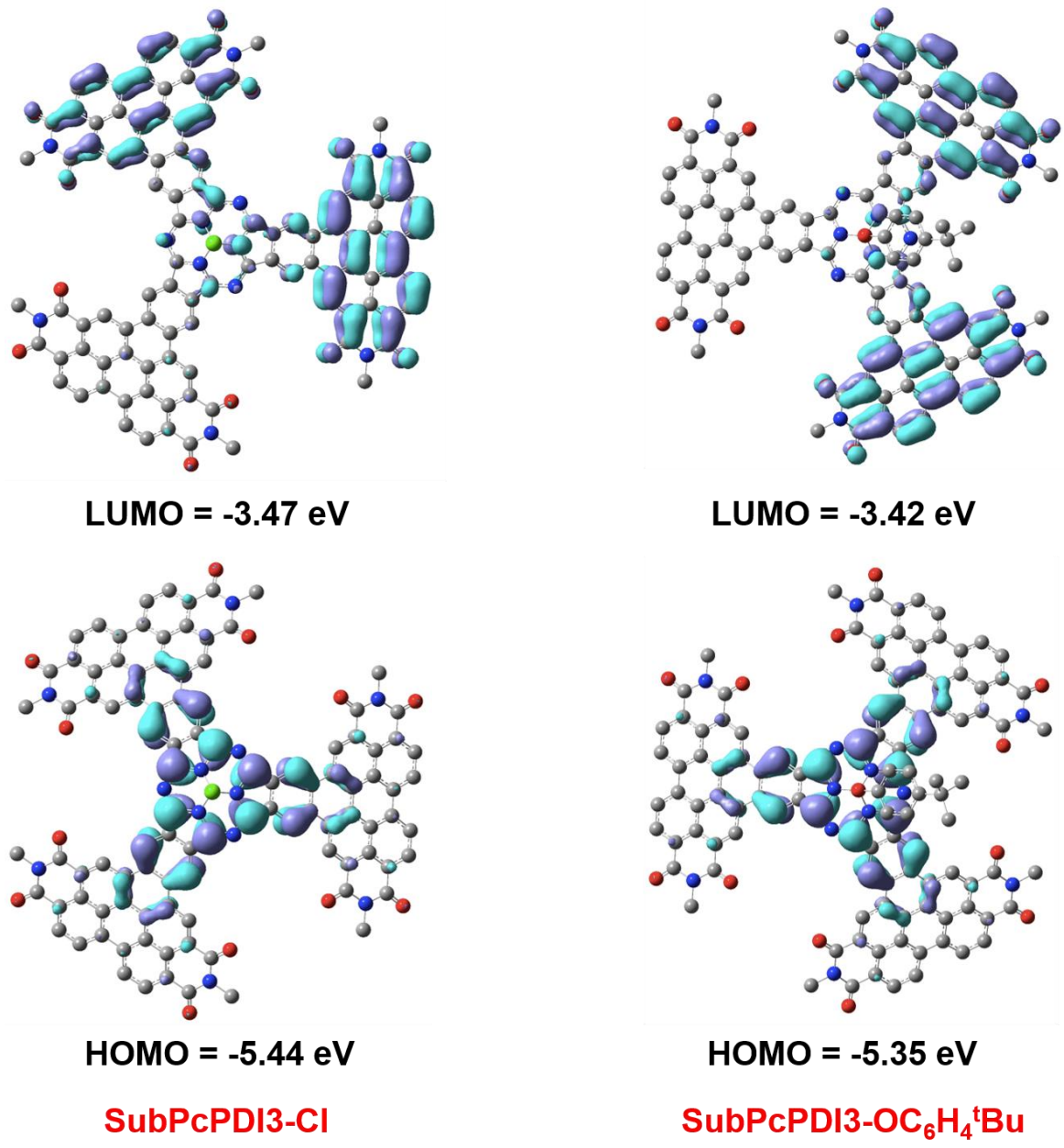

Figure S1. Frontier molecular orbitals of **SubPcPDI3-Cl** (left) and **SubPcPDI3-OC$_6$H$_4$^{t}Bu** (right).

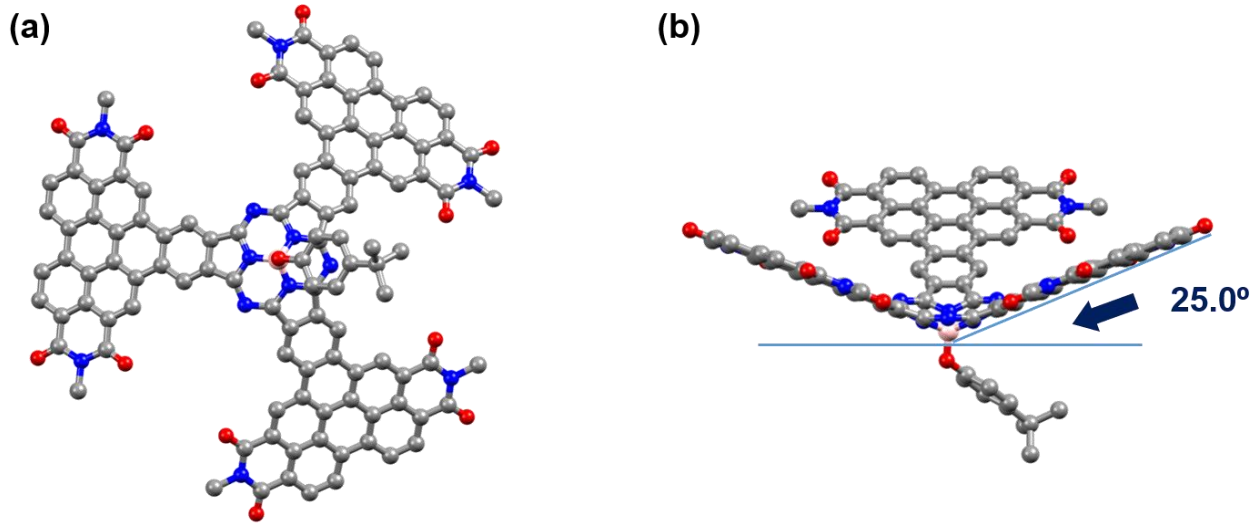

Figure S2. Top-view (a) and side-view (b) of **SubPcPDI3-OC$_6$H$_4$^{t}Bu**.

4. Photophysical Properties

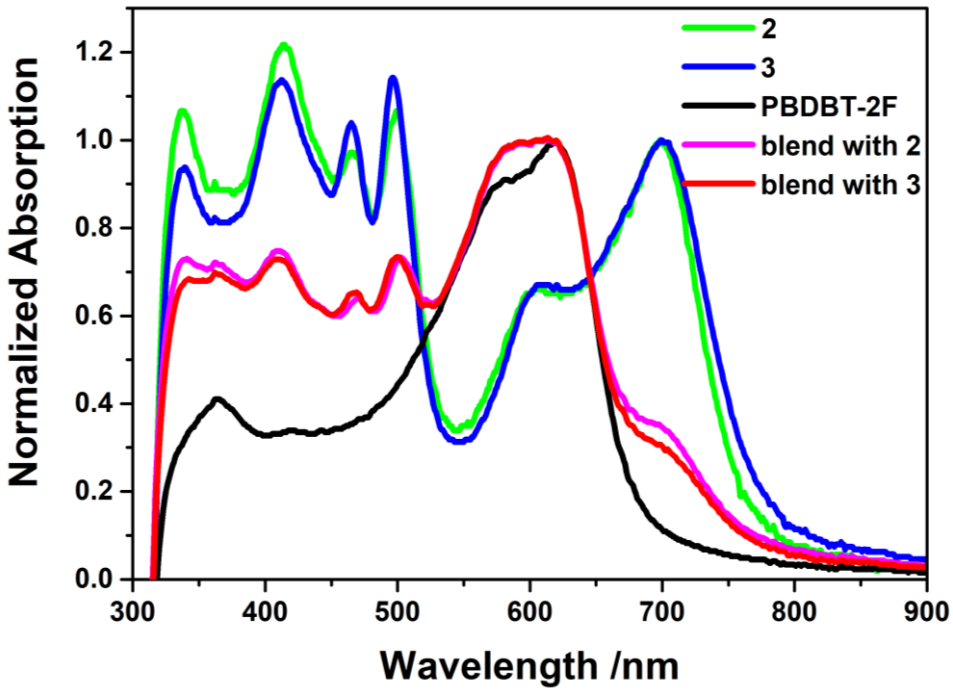

Figure S3. UV-vis absorption of the acceptor, donor and blends in films.

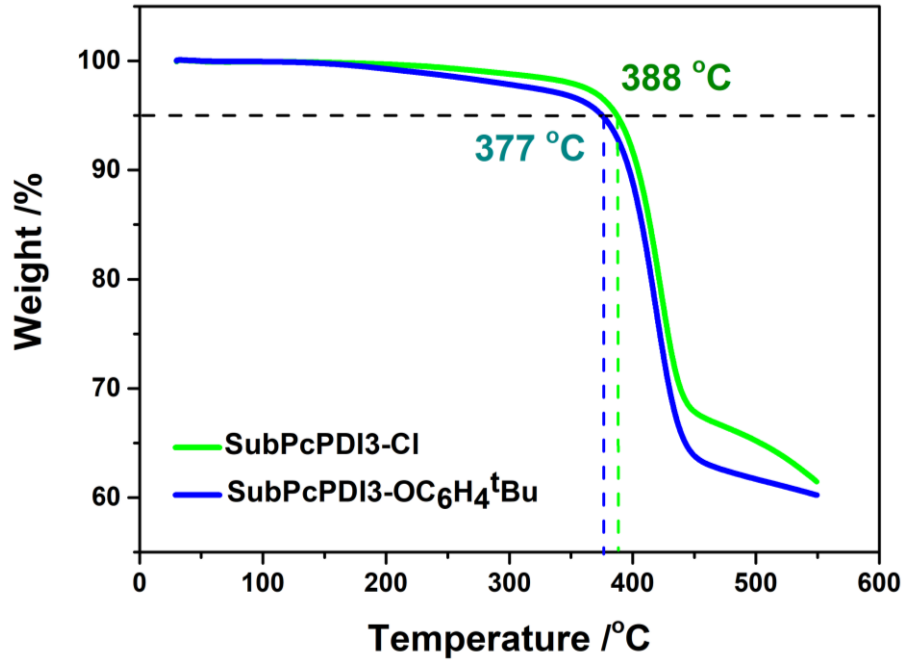

Figure S4. TGA curves of **SubPcPDI3-Cl** (green trace) and **SubPcPDI3-$OC_6H_4{}^tBu$** (blue trace).

5. Device Fabrication and Characterization

NF-PSCs Fabrication. The ITO substrates were sonicated sequentially in acetone, detergent, deionized water and isopropyl alcohol for cleaning the ITO surface, followed by drying at 90 °C for overnight in vacuum oven. ZnO interlayer from precursor solution was spin-coated onto the pre-cleaned and UV-treated ITO substrates, then heated at 200 °C for 1 hour. The device structures of ITO/ZnO/PBDBT-2F:acceptor/MoO_3/Ag was fabricated. The polymers and acceptors were co-dissolved in chlorobenzene (CB) with 1.0% DIO in volume fraction, at total solids concentration of 20 mg mL^{-1} and was stirred overnight at temperature of 70 °C. The active layer was spin-coated from the cooled blend solution obtain high neat films, the cast films were treated by thermal annealing at 100 °C for 10 mins. Subsequently, the resulted active films were transferred into a vacuum chamber. Afterwards, 10 nm molybdenum oxide (MoO_3) hole buffer and 100 nm Ag electrode was deposited by thermal evaporation through a defined shadow mask in a vacuum chamber with a pressure of approximately 1×10^{-4} Pa. The completed devices were tested in closed glove box.

Characterization of morpholgy. The film morphology was conducted by atomic force microscopy (AFM, Veeco Metrology Group/Digital Instruments) with tapping mode. Grazing incident wide-angle X-ray scattering (GIWAXS) measurements were performed at the 8ID-E beamline at the Advanced Photon Source (APS), Argonne National Laboratory using x-rays with a wavelength of λ = 1.1385 Å and a beam size of 200 µm (h) and 20 µm (v). A 2-D PILATUS 1M-F detector was used to capture the scattering patterns and was situated at 208.7 mm from samples.

Characterization of device. Steady-state current-voltage (*J-V*) curves were measured by a Keithley 2400 source-measurement unit under AM 1.5 G spectrum from a solar simulator (Enlitech.Inc) calibrated by a silicon reference cell (Hamamatsu S1133 color, with KG-5 visible fiith). The relationship of Jsc to the light intensity were measured by steady-state current-voltage measurement, the light intensity was modulated by neutral density filters (NDF) with different values of optical density (OD). The external quantum efficiency (EQE) was measured by a solar cell–photodetector responsibility measurement system (Enlitech. Inc). The mobility of electron was tested by fitting the current-bias characteristics in dark utilizing a field-independent space charge limited current (SCLC) model following the Mott-Gurney law given by $J = \frac{9}{8}\varepsilon_0\varepsilon_r\mu\frac{V^2}{L^3}$. The device structure for hole-only and electron-only devices are ITO/PEDOT:PSS/PBDBT-2F:acceptor/MoO_3/Ag and ITO/ZnO/PBDBT-2F:acceptor/PDINO/Al, respectively.

Table S1. The photovoltaic performance of the devices based on PBDB-T:**SubPcPDI3-Cl** with different additive content.

conditions	V_{OC} [V]	J_{SC} [mA cm^{-2}]	FF	PCE [%]
Cast	0.96	9.57 (9.41±0.14)	36.90 (36.42±0.44)	3.39 (3.26±0.12)
Cast+TA (100 °C)	0.96	11.03 (10.82±0.19)	37.03 (36.72±0.28)	3.92 (9.43±0.14)
0.5% DIO	0.97	12.92 (12.68±0.21)	46.20 (45.76±0.42)	5.80 (5.56±0.23)
0.5% DIO+TA (100 °C)	0.97	14.03 (13.86±0.18)	47.90 (47.38±0.49)	6.52 (6.31±0.20)
1.0% DIO+TA (100 °C)	0.97	14.10 (13.97±0.15)	55.04 (54.68±0.33)	7.53 (7.41±0.11)
1.5% DIO+TA (100 °C)	0.95	12.86 (12.57±0.28)	53.43 (53.05±0.37)	6.51 (6.33±0.17)

The parenthesis means the average value ± standard deviation calculated from 10 independent devices.

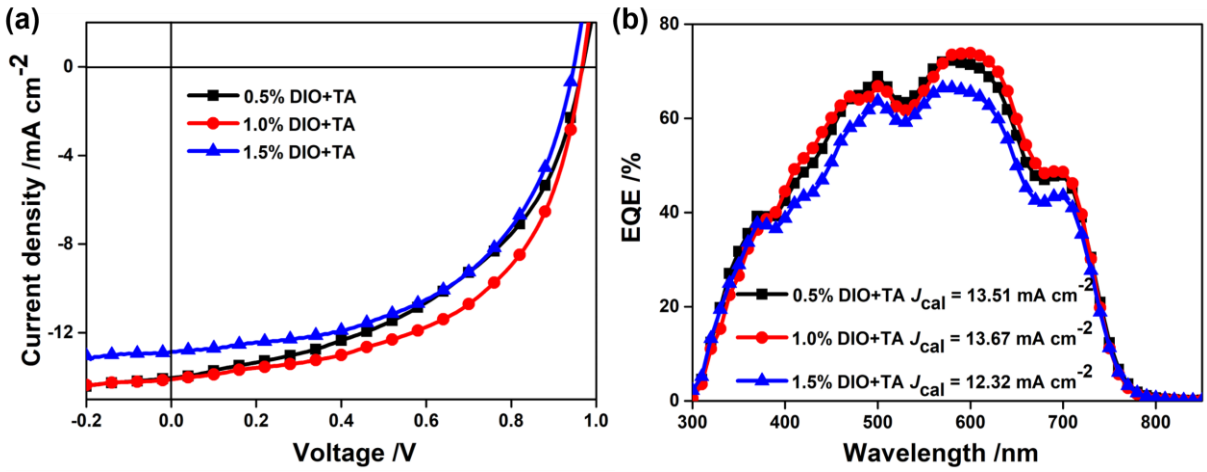

Figure S5. *J-V* characteristics of the devices based on PBDB-T:SubPcPDI3-Cl with different additive content (a) and corresponding EQE spectrum (b).

Table S2. Hole and electron mobilities of the optimized PBDBT-2F:acceptor blend films.

Acceptor	Hole Mobility ($cm^2\ v^{-1}\ s^{-1}$)	Electron Mobility ($cm^2\ v^{-1}\ s^{-1}$)	μ_h/μ_e
SubPcPDI3-Cl	$(4.3\pm0.16)\times10^{-5}$	$(2.7\pm0.25)\times10^{-5}$	1.6
SubPcPDI3-$OC_6H_4{}^tBu$	$(2.6\pm0.20)\times10^{-5}$	$(1.4\pm0.15)\times10^{-5}$	1.8

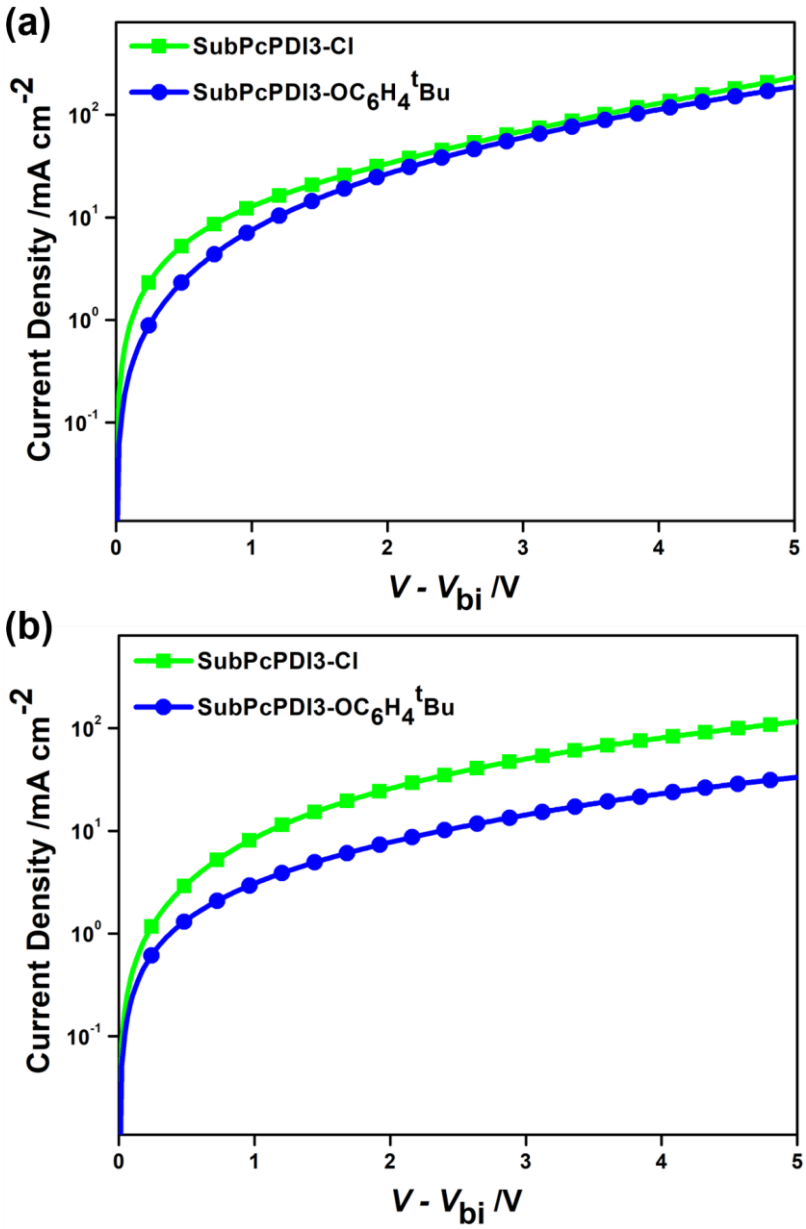

Figure S6. The experimental current density-applied voltage characteristics for hole-only devices (a) and electron-only devices (b) for PBDBT-2F:acceptor blend films.

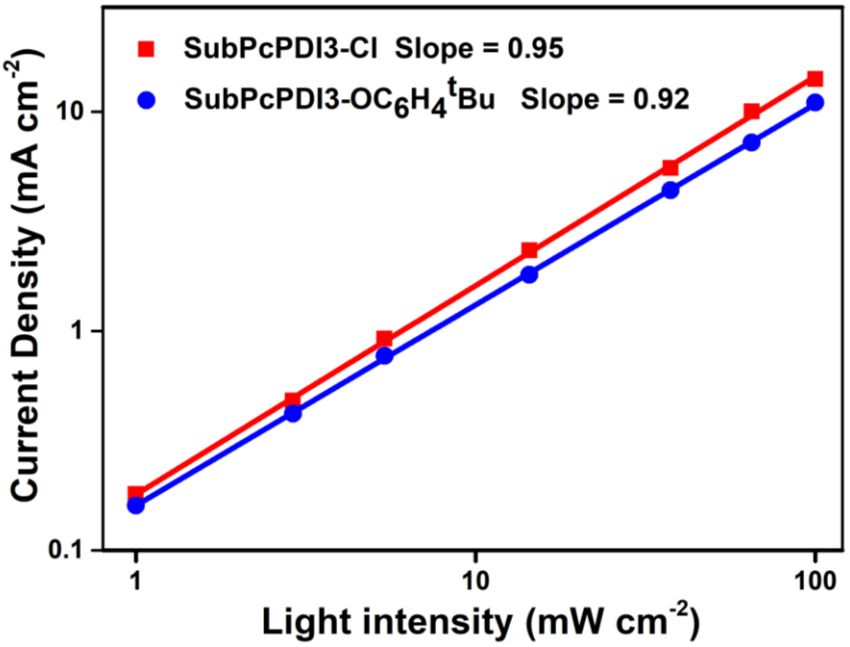

Figure S7. Dependence of J_{SC} on light intensity based on PBDBT-2F:acceptor devices.

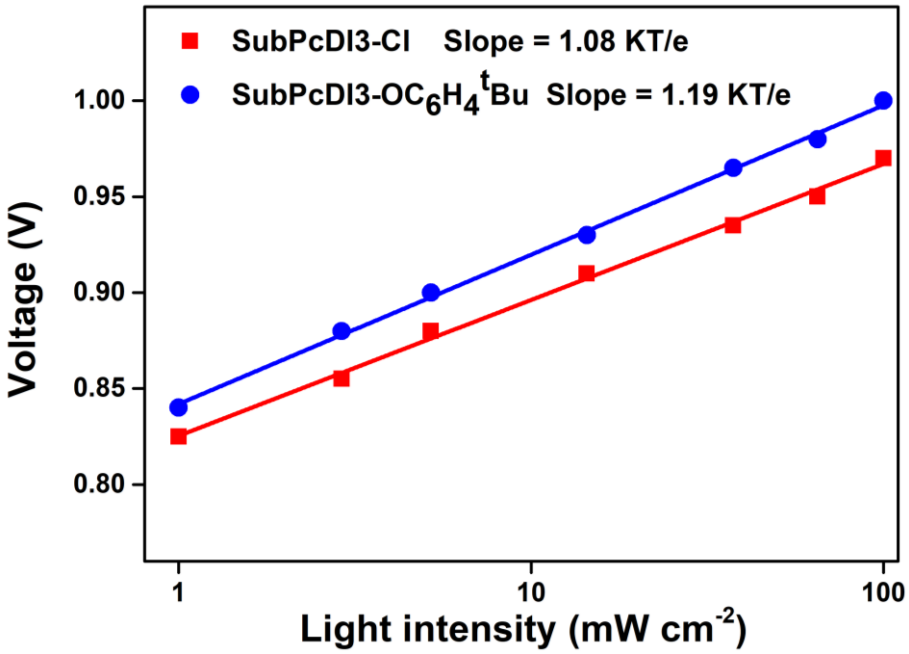

Figure S8. Dependence of V_{OC} on light intensity based on PBDBT-2F:acceptor devices.

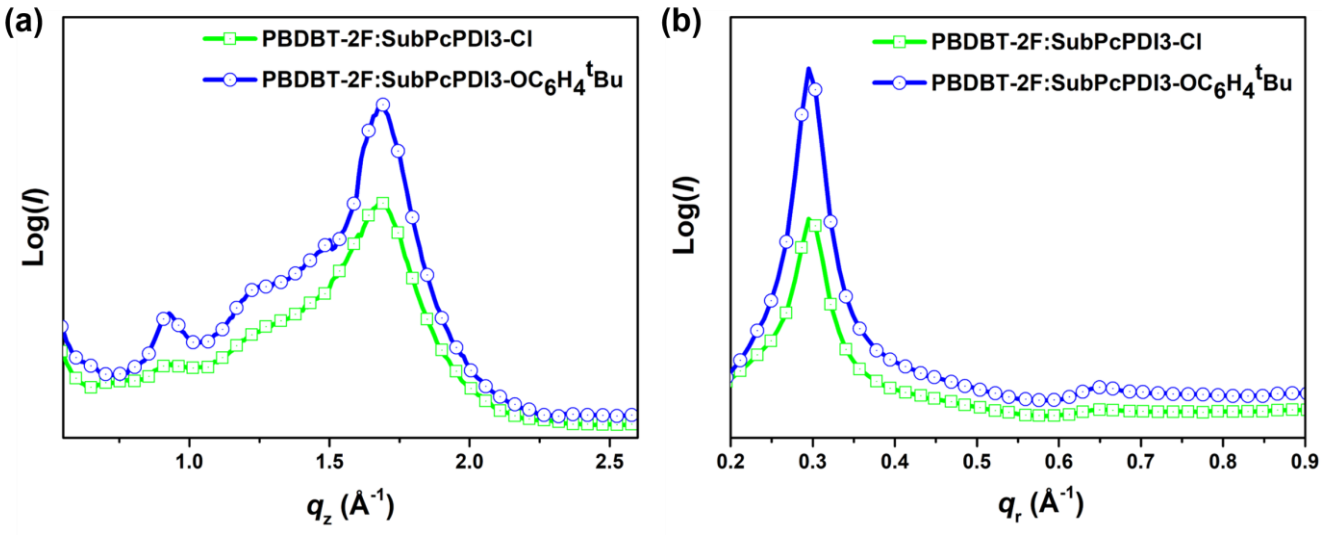

Figure S9. GIWAX line-cuts of PBDBT-2F:SubPcPDI3-Cl and PBDBT-2F:SubPcPDI3-$OC_6H_4{}^tBu$ blend films: in the out-of-plane (a) and in-plane (b).

6. References

[1] Gaussian 09, Revision E.01, M. J. Frisch, G. W. Trucks, H. B. Schlegel, G. E. Scuseria, M. A. Robb, J. R. Cheeseman, G. Scalmani, V. Barone, B. Mennucci, G. A. Petersson, H. Nakatsuji, M. Caricato, X. Li, H. P. Hratchian, A. F. Izmaylov, J. Bloino, G. Zheng, J. L. Sonnenberg, M. Hada, M. Ehara, K. Toyota, R. Fukuda, J. Hasegawa, M. Ishida, T. Nakajima, Y. Honda, O. Kitao, H. Nakai, T. Vreven, J. A. Montgomery, Jr., J. E. Peralta, F. Ogliaro, M. Bearpark, J. J. Heyd, E. Brothers, K. N. Kudin, V. N. Staroverov, T. Keith, R. Kobayashi, J. Normand, K. Raghavachari, A. Rendell, J. C. Burant, S. S. Iyengar, J. Tomasi, M. Cossi, N. Rega, J. M. Millam, M. Klene, J. E. Knox, J. B. Cross, V. Bakken, C. Adamo, J. Jaramillo, R. Gomperts, R. E. Stratmann, O. Yazyev, A. J. Austin, R. Cammi, C. Pomelli, J. W. Ochterski, R. L. Martin, K. Morokuma, V. G. Zakrzewski, G. A. Voth, P. Salvador, J. J. Dannenberg, S. Dapprich, A. D. Daniels, O. Farkas, J. B. Foresman, J. V. Ortiz, J. Cioslowski, and D. J. Fox, Gaussian, Inc., Wallingford CT, 2013.

7. NMR Spectra

^{1}H NMR spectrum of **2** (500 MHz, $CD_2Cl_2CD_2Cl_2$, 373 K)

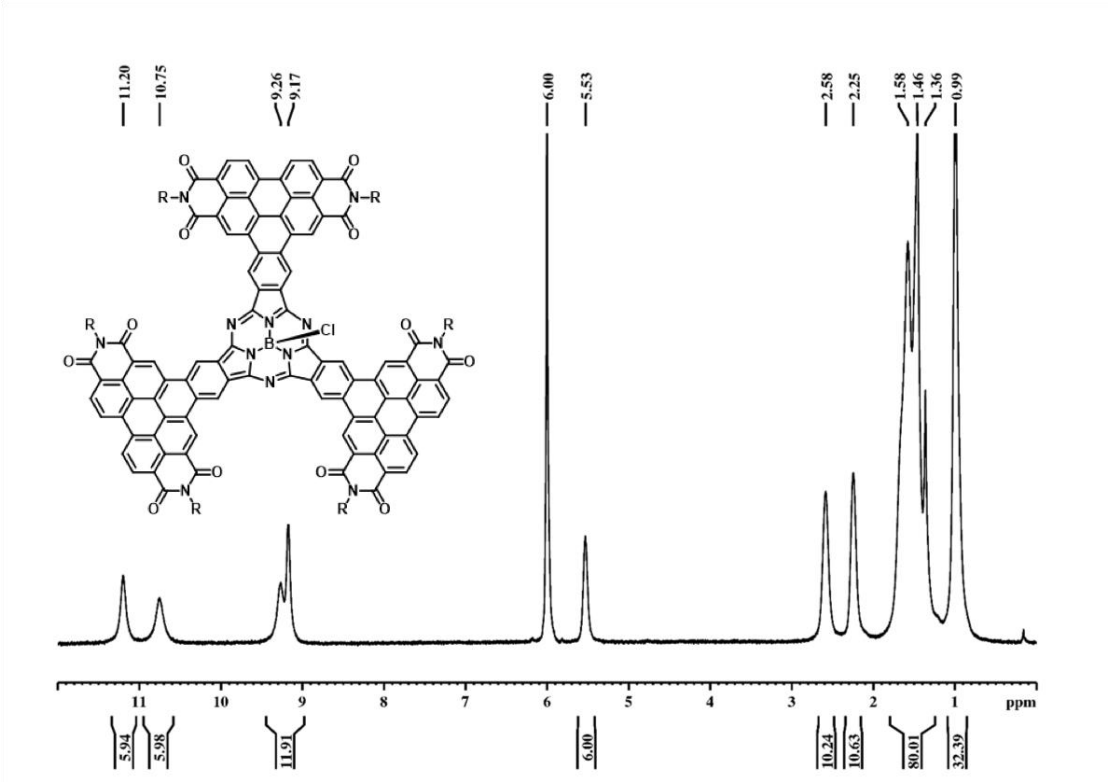

^{1}H NMR spectrum of compound **3** (500 MHz, $CD_2Cl_2CD_2Cl_2$, 373 K)

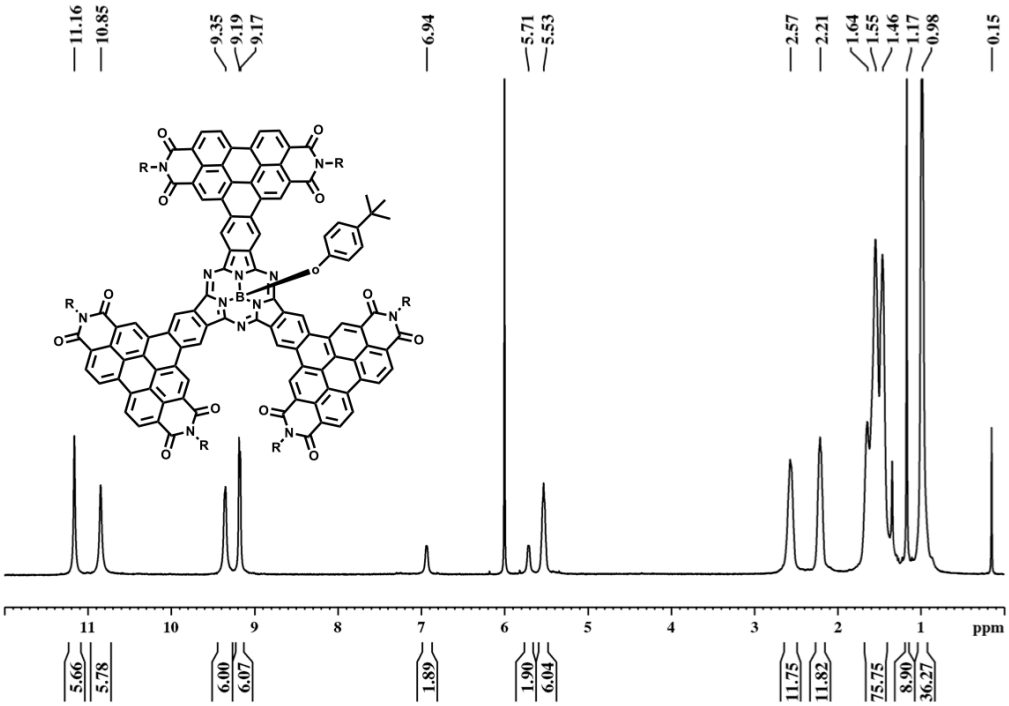

^{13}C NMR spectrum of compound **2** (125 MHz, $CD_2Cl_2CD_2Cl_2$, 373 K)

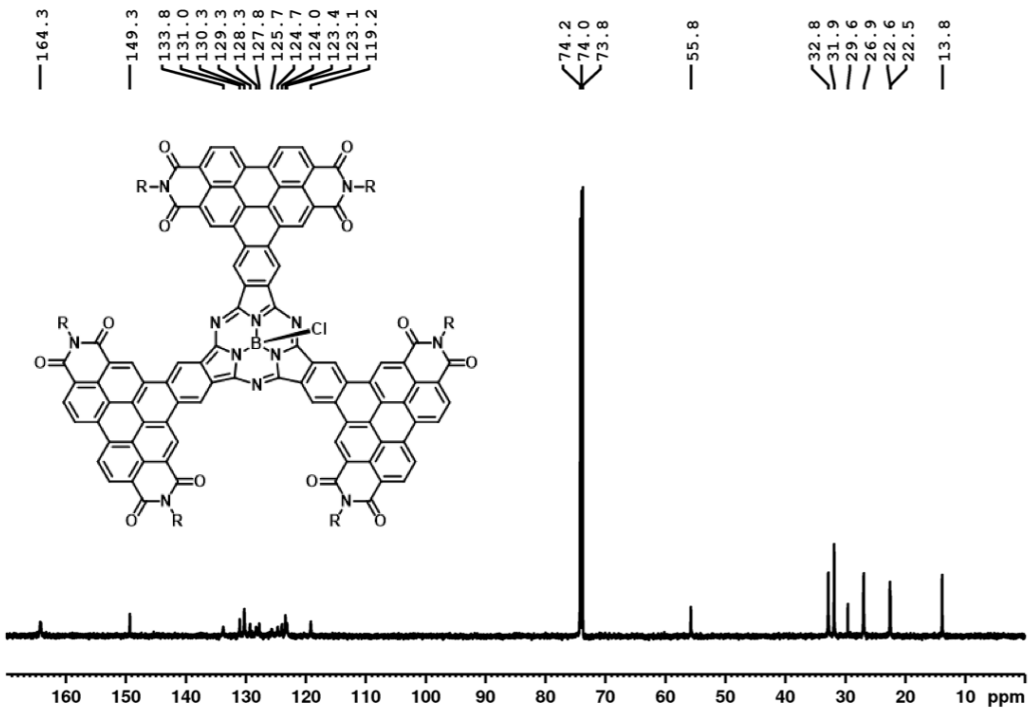

^{13}C NMR spectrum of compound **3** (125 MHz, $CD_2Cl_2CD_2Cl_2$, 373 K)